4. J. H. SCHMITT, J. M. JALINIER and B. BAUDELET, *J. Mater. Sci.* in press.
5. J. M. JALINIER, J. H. SCHMITT, R. ARGEMI, J. L. SALSMANN and B. BAUDELET, *Mem. Sci. Rev. Met.* 77 (1980) 313.
6. J. M. JALINIER, R. ARGEMI and B. BAUDELET, *J. Mater. Sci.* 13 (1978) 1142.
7. M. C. SOUZA NOBREGA, B. F. DA SILVA, G. FERRAN, J. M. JALINIER and B. BAUDELET, *Mem. Sci. Rev. Met.* 77 (1980) 293.
8. J. A. CHARLES and I. UCHIYAMA, *J.I.S.I.* 207 (1969) 979.
9. L. F. MONDOLFO, "Aluminium alloys – Structure and Properties" (Butterworth, London, 1976) pp. 814, 816, 837.
10. G. MESMACQUE, PhD thesis, University of Lille, France (1978).
11. A. INOUE, T. OGURA and T. MASUMOTO, *Trans. J. Inst. Met.* 17 (1976) 150.
12. F. MONTHEILLET, P. LEDERMANN and PERROT, *D.G.R.S.T. Rep.* (1979) to be published.
13. D. RAULT and M. ENTRINGER, private communication, (1980).
14. J. M. JALINIER and B. BAUDELET, 10th International Deep Drawing Research Group Meeting, Warwick, England, 1978 (Portcullis Press Ltd, Red Hill, England, 1978) p. 133.
15. Z. MARCINIAK and K. KUCZYNSKI, *Int. J. Mech. Sci.* 9 (1967) 609.
16. J. H. SCHMITT, D. Eng. Thesis, Metz, France (1981).

Received 15 October
and accepted 14 November 1980

J. H. SCHMITT
R. ARGEMI
J. M. JALINIER
B. BAUDELET
Laboratoire de Physique et Technologie des Matériaux,
Université de Metz,
57000 Metz,
France

Transverse cracks in glass/epoxy cross-ply laminates impacted by projectiles

Impacted composite laminates may fail with several different failure mechanisms either occurring separately or in some combination. In $[(0^\circ)_5/(90^\circ)_5/(0^\circ)_5]$ glass/epoxy cross-ply laminates impacted by cylindrical projectiles with different impactor nose shapes and lengths, a sequential delamination mechanism is dominant, initiated by a generator strip, of width approximately equal to the impactor diameter, cut from the first lamina by two through-the-thickness cracks parallel to the fibres of the first lamina [1]. Blunt-nosed projectiles produced clearer generator strips than hemispherical-nosed projectiles [2].

In addition, an observable, almost even distribution of fine transverse cracks in the 0° direction was noted on the front and back of the impacted plates in the 0° fibre direction, as shown in Fig. 1 for blunt-nosed projectiles. Some transverse cracks extend the full length of the specimen in the fibre direction, while others are combinations of several cracks. Similar transverse cracks in the middle, 90° orientated lamina can also be found along the fibre direction when the plates are illuminated by a strong back-light.

Similar types of transverse cracks with evenly distributed crack spacings in cross-ply laminates have been observed in different static loading conditions [3–12].

Recently, several authors have investigated in detail these characteristic transverse cracks in uniaxial tensile tests of cross-ply laminates and defined the factors controlling this evenly distributed crack spacing [13, 14]. Garrett and Bailey [13] have found the spacing of transverse cracks to be dependent both on the thickness of the transverse ply and on the applied stress. Generally, the higher the applied stress and the smaller the transverse ply thickness are, the smaller is the average crack spacing. The above discussion on transverse cracking relates mainly to static tensile tests but can be applied directly to transverse cracking in the impacted laminates in a qualitative manner as follows.

In order to do this, the crack spacing on the front and back faces of each lamina of each specimen was measured and the arithmetic mean was then calculated. The mean transverse crack distance (MTCD) was found as a function of impactor velocity and is shown in Fig. 2 for five impactor types. The two marks for each specimen correspond to the MTCD measured on the front and back laminas, respectively. For blunt-nosed impactors (Fig. 2a), the upper points correspond to the

0022–2461/81/072008–04$02.40/0

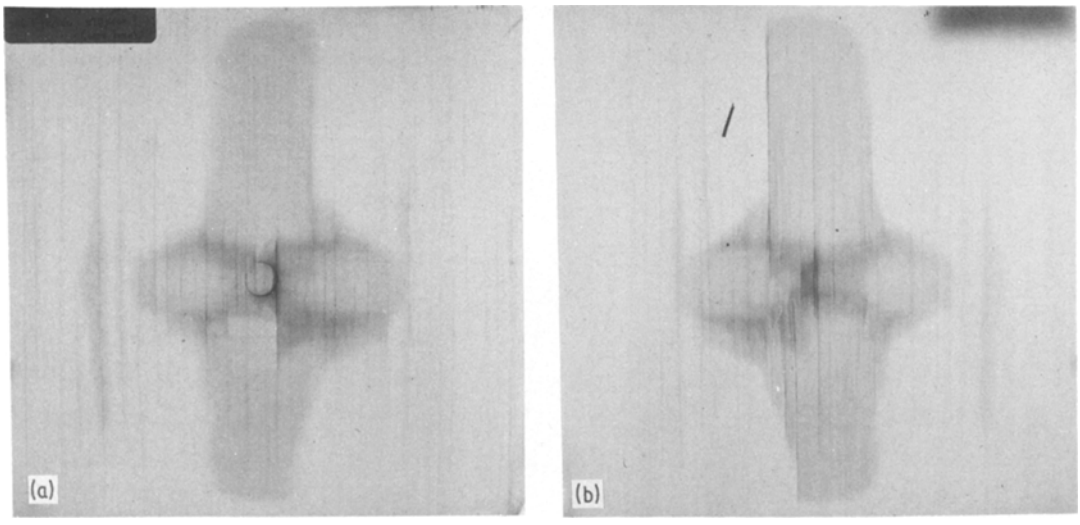

Figure 1 Failure appearance of $[(0°)_5/(90°)_5/(0°)_5]$ glass/epoxy laminates impacted by a blunt-nosed projectile. (a) Front view; (b) back view.

MTCD measurements on the back lamina and the lower points correspond to the MTCD measurements on the front lamina; that is, for blunt-nosed impactors and for a given impactor velocity, the MTCD was found to be smaller at the front lamina of a plate than at the back. For hemispherical-nosed and truncated hemispherical-nosed impactors (Fig. 2b and c, respectively), the reverse was found. That the impact energy is more widely dissipated at the front lamina with blunt-nosed impactors than with hemispherical-nosed impactors is an interesting indication of nose-shape effects.

The threshold impactor velocity, v_T, for the development of the transverse cracks appears to be independent of impactor type and to be about 23 m sec^{-1}. Above this threshold velocity, the MTCD decreases sharply as the impactor velocity increases. The curves are eventually flattened out at higher velocities and the MTCD appears to reach its minimum value, found to be approximately 3 mm for the $[(0°)_5/(90°)_5/(0°)_5]$ specimens. This is similar to the MTCD against applied stress curve in static tensile tests of cross-ply laminates reported by Garrett and Bailey [13]. Although different nose shapes can result in a difference in the MTCD on the front and back surfaces, change in nose shape does not lead to any differences in the other observed characteristics of the curve.

Long (5.08 cm) impactors produce larger MTCD values than do short impactors (2.54 cm) at the lower velocities but the impactor length (mass) has little effect on MTCD values at higher velocities.

The front and back surfaces of impacted plates of $[(0°/90°)_7/0°]$ and $[(0°)_3/(90°)_3/(0°)_3/(90°)_3/(0°)_3]$ laminate configurations show the same uniform transverse crack development as for the $[(0°)_5/(90°)_5/(0°)_5]$ ones. Some MTCD data for each impacted plate type have also been shown in Fig. 2a. The MTCD values increase in the order of the listing of the three laminate configurations, i.e. with smallest MTCD values obtained for the $[(0°/90°)_7/0°]$ laminate, while the threshold velocity for transverse crack development decreases in the order of listing.

In the impact experiments, the laminate specimen may experience deflections comparable to or larger than the plate thickness so that membrane effects may have to be considered. The well-known von Kármán theory for the large deflections of plates (see, for example [15]) makes use of Green's finite strain as follows. In the Lagrangian description, two components of the Green's strain tensor, E_{xx} and E_{yy}, referring to the initial configuration, are

$$E_{xx} = \frac{\partial u}{\partial x} - z\frac{\partial^2 w}{\partial x^2} + \frac{1}{2}\left(\frac{\partial w}{\partial x}\right)^2; \quad (1)$$

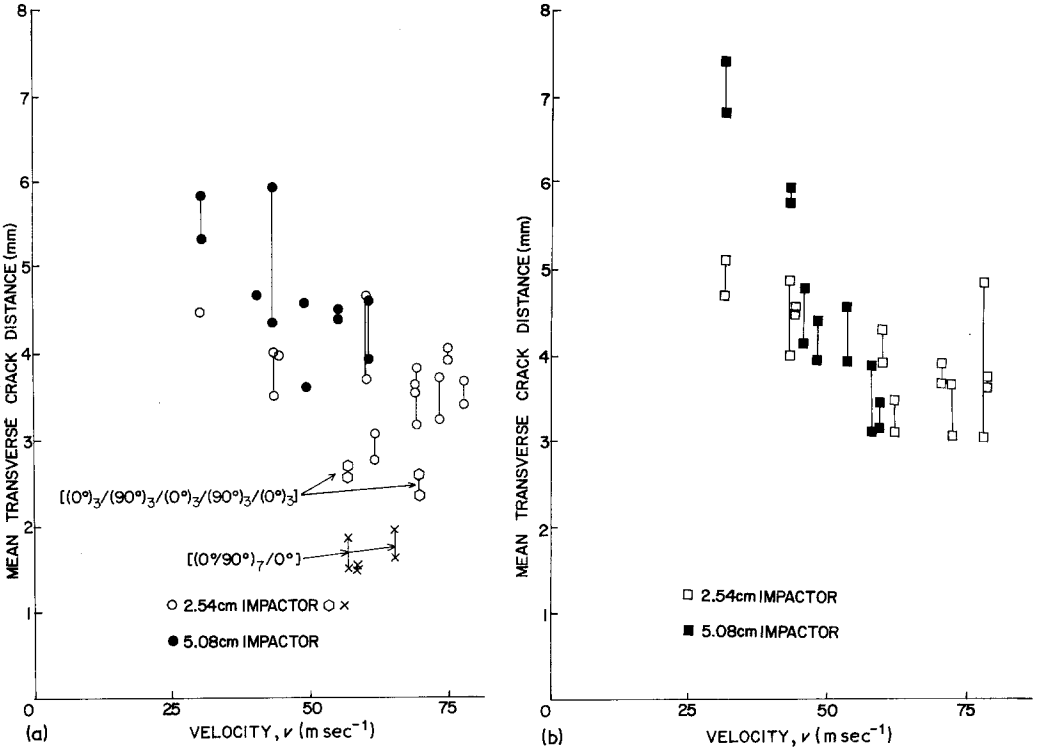

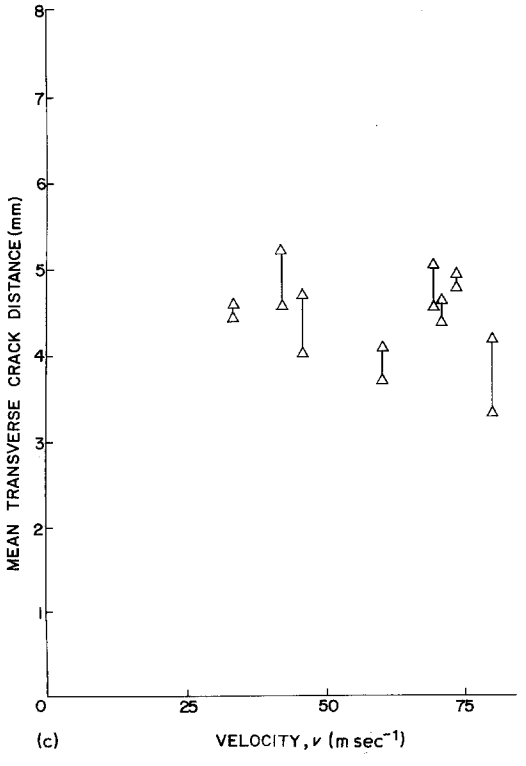

Figure 2 Mean transverse crack distance plotted against impactor velocity for $[(0°)_5/(90°)_5/(0°)_5]$ laminates impacted by various types of impactors. Some data for other laminates are included for comparison. (a) Blunt-nosed impactor. Paired points: upper for back face, lower for front face. (b) Hemispherical-nosed impactors. Paired points: lower for back face, upper for front face. (c) Truncated hemispherical-nosed impactors (2.54 cm). Paired points: lower for back face, upper for front face.

and

$$E_{yy} = \frac{\partial v}{\partial y} - z\frac{\partial^2 w}{\partial y^2} + \frac{1}{2}\left(\frac{\partial w}{\partial y}\right)^2; \qquad (2)$$

where u and v are in-plane displacements in the x and y directions while w is the plate deflection. The first term in both Equations 1 and 2 can be small compared with the other terms. The second term is the contribution of bending which also exists in the small-deflection theory. The third term is particular to the large-deflection theory and may be comparable in magnitude to the second term. This term contributes a membrane tensile component to the strain and causes transverse cracking in transverse laminas. A theoretical explanation developed by Garrett and Bailey [13] from static tensile test data, i.e. a modified shear

lag analysis, can be applied to explain this transverse cracking in cross-ply laminates, with some changes to account for wave propagation effects; however, the development of this approach requires further work.

Acknowledgement

The authors wish to acknowledge the U.S. Army Research Office, Durham, NC, for their support of this research programme under Grant No. DAAG29-79-G-0007.

References

1. N. CRISTESCU, L. E. MALVERN and R. L. SIERAKOWSKI, "Foreign Object Impact Damage to Composites", ASTM STP 568 (ASTM, Philadelphia, 1975) p. 159.
2. N. TAKEDA, R. L. SIERKOWSKI and L. E. MALVERN, *SAMPE Quart.* **12** (1981) 9.
3. L. J. BROUTMAN, "Modern Composite Materials", edited by L. J. Broutman and H. Krock (Addison-Wesley, New York, 1967) Chap. 13.
4. H. T. HAHN and S. W. TSAI, *J. Comp. Mater.* **8** (1974) 288.
5. J. BAX, *Plast. Polymers* **38** (1970) 27.
6. M. L. C. JONES and D. HULL, *J. Mater. Sci.* **14** (1979) 165.
7. K. L. REIFSNIDER, E. G. HENNEKE and W. W. STINCHCOMB, Proceedings of the 4th International Conference on Compositie Materials: Testing and Design, ASTM STP 617 (ASTM, Philadelphia, 1977) p. 93.
8. K. L. REIFSNIDER and A. TALUG, Proceedings of the Research Workshop on Mechanics of Composite Materials, (Duke University, Durham, NC, 1978) p. 130.
9. J. A. KIES, U.S. Naval Research Lab. Report Number 5752 (1962).
10. J. C. SHULTZ, 18th Annual Conference of the SPI Reinforced Plastics Division Sec. 7-D February, 1963.
11. L. R. HERRMANN and K. S. PISTER, ASTM Paper 62-WA-239 (1963).
12. A. PUCK and W. SCHNEIDER, *Plast. Polymers* **37** (1969) 33.
13. K. W. GARRETT and J. E. BAILEY, *J. Mater. Sci.* **12** (1977) 157.
14. G. T. STEVENS and A. W. LUPTON, *ibid* **12** (1977) 1706.
15. Y. C. FUNG, "Foundations of Solid Mechanics" (Prentice-Hall, Inc., Englewood Cliffs, NJ, 1965) p. 463.

Received 15 October
and accepted 14 November 1980

N. TAKEDA*
R. L. SIERAKOWSKI
L. E. MALVERN
Department of Engineering Sciences,
University of Florida,
Gainesville,
Florida 32611,
USA

*Present address: Institute of Space and Aeronautical Science, University of Tokyo, Komaba, Tokyo, Japan.

Electrical conduction in $Na_3H(SO_4)_2$ and $(NH_4)_3H(SO_4)_2$ crystals

Electrical transport in hydrogen-bonded lattices like potassium dihydrogen phosphate (KDP), potassium hydrogen sulphate etc. has been systematically and widely studied and it has been established beyond doubt that the charge carriers are protons [1–6]. Trisodium hydrogen sulphate is a hydrogen-bonded system. Infrared absorption studies [7] as well as X-ray crystal structure determination [8] have shown the presence of a HSO_4^- group in trisodium hydrogen sulphate. Electrical conductivity and dielectric loss measurements have been undertaken on $Na_3H(SO_4)_2$ crystals to investigate the mechanism of electrical transport in the lattice. The studies have been extended to the isostructural $(NH_4)_3H(SO_4)_2$ crystals.

Single crystals were grown by slow evaporation of saturated aqueous solutions of $Na_3H(SO_4)_2$ and $(NH_4)_3H(SO_4)_2$. $Na_3H(SO_4)_2$ crystals doped with iron were grown by adding a few drops of ferric sulphate solution to the original solution. The composition of $Na_3H(SO_4)_2$ was checked by comparing the Debye–Scherrer powder diffraction data with ASTM data cards [9, 10]. Electrical conductivity measurements were carried out under 10^{-2} Torr vacuum using a GR 1230 d.c. electrometer/Keithley 610C solid state electrometer. The dielectric loss measurements were carried out on a GR 1620 AP capacitance measuring bridge assembly in the temperature range 60 to 130° C and in

